Quaternary Geochronology 50 (2019) 8–13

Contents lists available at ScienceDirect

Quaternary Geochronology

journal homepage: www.elsevier.com/locate/quageo

^{10}Be exposure ages for the Late Pleistocene Gour de Tazenat maar (Chaîne des Puys volcanic field, Auvergne, France)

Greg A. Valentine[a,*], Jason P. Briner[a], Benjamin van Wyk de Vries[b], Élodie Macorps[c], Dale Gump[a]

[a] Department of Geology, 126 Cooke Hall, University at Buffalo, Buffalo, NY, 14260, USA
[b] Université Clermont Auvergne, CNRS, IRD, OPGC, Laboratoire Magmas et Volcans, F-63000, Clermont-Ferrand, France
[c] School of Geosciences, 4202 E. Fowler Avenue, NES 107, University of South Florida, Tampa, FL, 33620-5550, USA

ARTICLE INFO

Keywords:
^{10}Be
Exposure dating
Maar
Massif central
Chaîne des Puys

ABSTRACT

Gour de Tazenat is a maar volcano on the crystalline Plateau des Domes, the uplifted margin of the Limagne Rift of the Massif Central of France, and forms one of the northernmost volcanic centers of the Chaîne des Puys volcanic field. Although long recognized as a relatively young volcanic center in the area, age determinations have been elusive, with the only one quantitative estimate based upon radiocarbon ages of bulk sediments in the crater lake and extrapolation of sedimentation rates to account for the full thickness of the sediments; that age is ~35 cal ka. Here we test application of cosmogenic ^{10}Be exposure dating to quartz-bearing subvolcanic rocks exposed in the wall of the maar crater. Considering erosion rates (~5 m/Myr) that we determined from ^{10}Be data on a nearby tor (located outside the crater), and corroborated by inverted relief of older, dated lavas in the region, the ^{10}Be data yield an age of 29–34 ka for the maar-forming eruption of Gour de Tazenat. This is consistent with the one previous quantitative estimate, and provides confidence in the age range of the maar. This age corresponds to a pulse of volcanic activity around 30 ka in other parts of the Chaîne des Puys.

1. Introduction

Quantitative age determinations for late Quaternary maar volcanoes can in some cases be obtained from organic material buried by eruption products, by methods such as luminescence and $^{40}Ar/^{39}Ar$ applied to juvenile tephra if its composition is amenable to these techniques, and by dating the lowermost crater fill sediments to give a minimum age (e.g., Preusser et al., 2011; Chassiot et al., 2018). In many cases these approaches do not work, for example if the eruption occurred in an arid or semi-arid climate with little vegetation, or if juvenile material is sparse. Surface exposure dating using cosmogenic nuclides can also be challenging because the eruptive products are typically loose tephras and the deposit surfaces are easily modified (e.g., Sasnett et al., 2012). However, since maar volcanoes by definition have craters that cut into the pre-eruptive landscape, exposures of pre-eruptive rocks in a crater wall, if competent and resistant to erosion, may provide opportunities for exposure dating. For example, Valentine et al. (2017) attempted to determine the exposure age of silicic ignimbrite exposed in the wall of Lunar Crater maar (Nevada, USA) by analysing ^{10}Be in quartz from those rocks. This provided information that, combined with age data from lavas cut by crater formation, allowed bracketing of the maar eruption age that was otherwise not quantifiable. Such data not only aid in dating volcanic events, but also can be combined with additional cosmogenic nuclide data to determine landscape evolution rates.

Here we apply ^{10}Be dating to outcrops of pre-volcanic rocks within the Late Pleistocene Gour de Tazenat maar, part of the Chaîne des Puys volcanic field (Massif Central, France). This young maar has eluded quantitative age determination, although data from sediment cores in its crater lake (Juvigné and Stach-Czerniak, 1998) allowed determination (radiocarbon) of a minimum crater age and an estimate of the absolute age. We dated silicic rocks exposed within the crater, correcting for local erosion rates calculated from ^{10}Be data from a tor of similar lithology in the surrounding terrain; the latter are consistent with estimated long-term exhumation rates in the region based upon inverted relief of older lava flows.

2. Regional and physiographic setting

The Gour de Tazenat maar (*gour* means deep hole) is at the extreme northern end of the Chaîne des Puys volcanic field (Boivin et al., 2009, 2017), on the Plateau des Domes, a raised margin of the Limagne Rift (Fig. 1). The entire region, including the rift basin, experienced Quaternary uplift following the cessation of major Oligocene-Miocene extension. Gour de Tazenat is isolated from other volcanoes at the

* Corresponding author.
E-mail address: gav4@buffalo.edu (G.A. Valentine).

https://doi.org/10.1016/j.quageo.2018.11.002
Received 20 July 2018; Received in revised form 14 November 2018; Accepted 15 November 2018
Available online 16 November 2018
1871-1014/

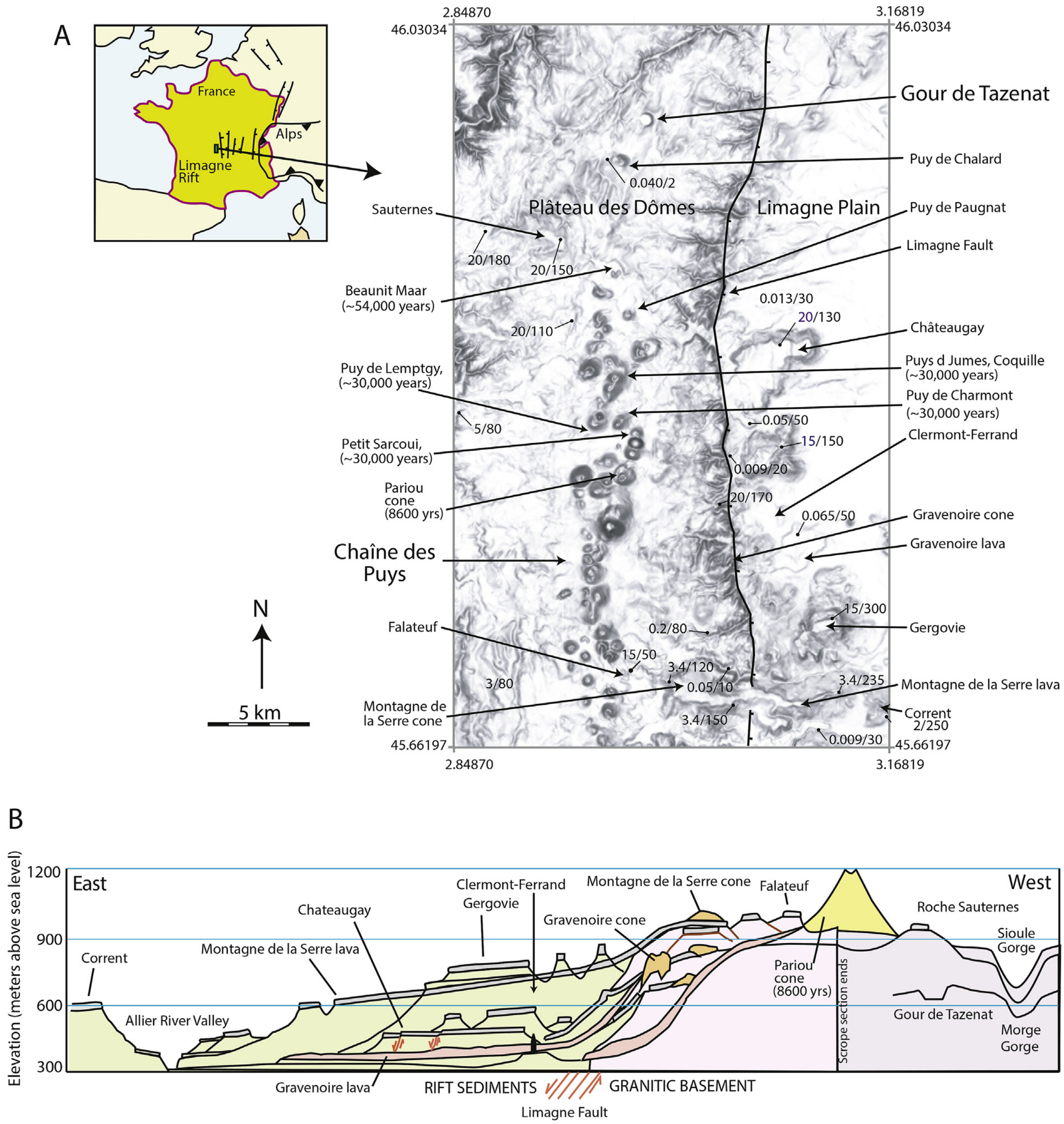

Fig. 1. Regional context of the Gour de Tazenat with respect to the Chaîne des Puys volcanic field and the Limagne fault. **A.** Map showing the location of the Gour de Tazenat in the context of the Limagne Rift, with the Limagne Fault, Chaîne des Puys volcanic field and the various inverted relief lava plateaux indicated (inset shows location in France). Numbers refer to ages (Myr) and topographic inversion (m) for lava mesas in the Chaîne des Puys (for example, 20/130 means the lava age is 20 Myr, and it now stands 130 m above the surrounding terrain). **B.** Schematic cross section modified from Scrope (1825, Plate XVII), showing the combined profiles of various lava flows and their inverted relief, from the youngest (in the deep valleys) to the oldest, perched on ridges standing above the Plateau des Domes and the Limagne rift plain. Note that in keeping with Scrope's original diagram, the cross section is presented as if viewed from the north, such that west is to the right and east to the left. The vertical line marked "Scrope section ends" is where two of his original cross sections are placed together (one section was to the east of Pariou cone, the other to the west of the cone).

northern end the Chaîne des Puys, with just one nearby scoria cone 2 km to the south-southeast (Figs. 1 and 2). The maar lies in an area of crystalline Hercynian basement (Manzat-St. Pardoux granites) that is overlain by a lower Carboniferous ignimbrite sequence (Manzat Formation; Jeambrun et al., 1986). The ignimbrites are crystal-rich, welded, and contain fragments of lavas, tuffs, microgranites, siltstones and shales. The Manzat Formation is intruded by 10's of m-wide microgranite dykes (Jeambrun et al., 1986). There is a strong brittle structural grain, with shear zones crossing the areas in a NNE-SSW direction (Late Hercynian faults), a direction paralleled by the dykes (Fig. 2).

To the south of Gour de Tazenat crater, the plateau is topped in several places by Miocene to Quaternary lava flows, which are also found straddling the Limagne fault – the main rift-bounding normal fault in the area – and in many cases extending into the rift valley (Fig. 1b). The lavas were originally emplaced onto the valley floor but now form inverted relief features due to exhumation of older country rock (on the plateau) and of poorly consolidated rift-fill sediments (in the rift) that surround them. The resulting mesas provide relative paleo-elevations of the ground surface at the emplacement time of each lava.

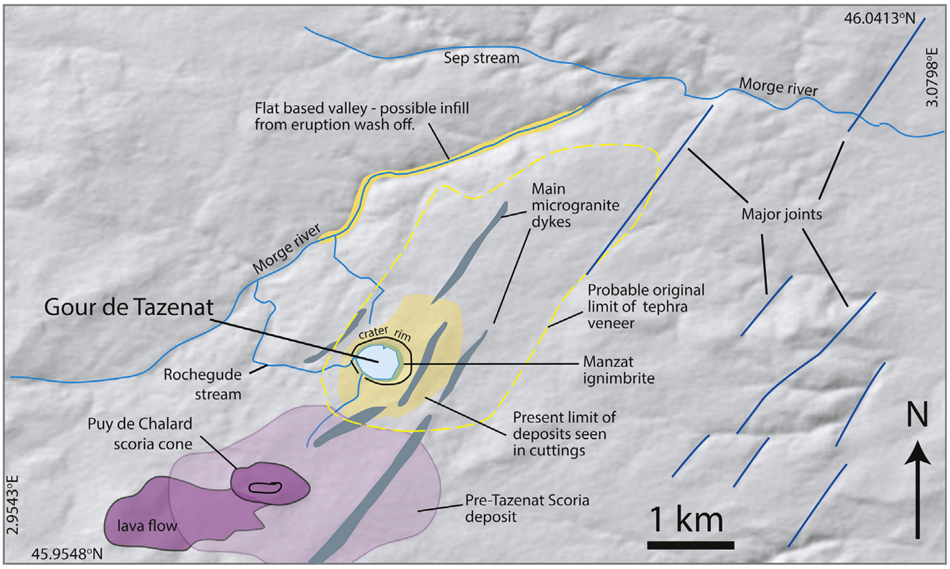

Fig. 2. Shaded relief image of the Plateau des Domes around Gour de Tazenat, including the Morges river valley to the north and major joint systems that are associated with the Limagne fault. Key geologic features discussed in the paper include major joints, micrognaritic dikes (blue-gray), the nearby cone (Puy de Chalard) and its lavas (purple), exposure of Manzat Formation ignimbrite within the crater (light green), and the inferred original and modern extents of the Tazenat deposits (yellow).

These relationships have been used since the 18th Century to provide information about uplift and exhumation, as evidence of broad scale geological processes such as uniformitarianism and the origin of volcanoes (e.g. Desmarest, 1774; Scrope, 1825).

The land surface around Gour de Tazenat is a gently rolling plateau, truncated 10 km to the east by the ~N-S trending Limagne fault escarpment, and sloping towards and dissected to the west and north by the Morge river valley (Fig. 2). Ridge crests align with the NNE-SSW-trending microgranite dikes such as those immediately southeast and northwest of the crater. The intervening valleys are cut into the Manzat Formation and often follow basement fracture sets.

Gour de Tazenat maar formed in the bend of the small Rochegude stream that joins the Morge river downstream. The Morge valley has a flat base from this point for 5 km downstream to a confluence, and a V-shaped incised profile upstream of that (Fig. 2). The local flat base of the valley is likely due to infilling by reworked tephra associated with the Tazenat eruption. For about 1–2 km to the northeast of the maar, the plateau has a relatively smooth surface due to deposition of tephra from the maar-forming eruption. Southwest of the crater, Rochegude stream flows through a broad valley that is itself covered by tephra from the nearby scoria cone.

The maar has a slightly elliptical crater with a 630 m short axis at N145°, and a 690 m long axis at N35°. It hosts a 66-m-deep lake underlain by at least 15 m of lacustrine sediments that rest upon the diatreme top (Juvigné and Stach-Czerniak, 1998). The north-northeastern part of the crater has a high and steep-sided rim sloping down at 20° to 30° from 710 m to 640 m a.s.l. at the surface of the lake. The lowest ~20 m of the exposed crater wall, above lake level, consists of jointed Manzat Formation rocks, while the upper ~50 m consists of basaltic tephra from the maar-forming eruptions (Fig. 2). It is likely that NNE-directed winds during the eruptions caused the thick accumulation of tephra on this side of the crater. The height of the eastern rim of the crater is due to a combination of tephra and a basement high formed by the microgranitic dike along its east-southeastern side (Fig. 2). In contrast to the east-northeast side, the southwestern half of the crater has a low and flat rim rising only ~15 m above lake level, except near the outflow stream where there are lower slope angles.

3. Previous geochronology studies

Gour de Tazenat has been noted to be a relatively young structure within the Chaîne de Puys volcanic field, ever since geologists came to the region (e.g., Scrope, 1825; Glangeaud, 1913). The first attempt at a date was simply by qualitative analogy to other landforms and tephras in the Chaîne des Puys, by Camus et al. (1983), who placed the age at a few tens of kyr. Thermoluminescence dating of silicic basement xenoliths within the tephra was attempted by Pilleyre (1991), who reported ages of 45 and 125 ka, but was not successful in reducing errors, possibly due to underheating of the xenoliths by the magma. He nevertheless estimated an age of several tens of kyr as well.

Three radiocarbon ages from bulk sediments in a lake sediment core provide a rudimentary age-depth model that allows for a crude extrapolation to the core base (Juvigné and Bastin, 1995). The oldest level dated, at ~9.9 m depth, is 13,730 ^{14}C yr BP (~16,585 cal yr BP). Extrapolation to the core base at ~14 m, believed to be the contact between volcanic breccia and lacustrine sediments, results in an estimated basal age of ~35 cal ka for the lake sediments (Juvigné and Bastin, 1995; Juvigné and Stach-Czerniak, 1998). There is no evidence for vastly different sedimentation below the lowest dated interval (e.g., turbidites) and thus a simple extrapolation seems reasonable, even if just a first-order approximation.

4. Sample setting, methods, and results

Sampling for ^{10}Be analysis was conducted on Manzat Formation exposures on the maar crater wall (Fig. 3a; Table 1) with the aim of determining an age for the crater, and on a tor associated with a microgranite dike 250 m northwest of the crater, in order to obtain an estimate of erosion rates that might lead to corrections in the crater wall ^{10}Be ages. At all sites, care was taken to sample from nearly flat-lying outcrop surfaces on the generally inward sloping crater, and the horizon was surveyed in order to account for topographic shielding effects on ^{10}Be production in the sample surfaces (Fig. 3b and c). All samples were of silicic composition, providing quartz for ^{10}Be analysis. Quartz was separated and digested, and ^{10}Be isolated and purified, at the University at Buffalo following established procedures (Kohl and Nishiizumi, 1992; Corbett et al., 2016).

Beryllium-10 is produced in quartz ~98% by spallation via neutrons, and the remaining by fast and slow muons [see Heisinger et al. (2002a, 2002b). Beryllium ratios (^{10}Be/^{9}Be) were measured at the Purdue Rare Isotope Measurement Lab. Ages were calculated using the CRONUS-Earth online calculator (Balco et al., 2008; version 3; http://hess.ess.washington.edu/math/) using Lm scaling (Lal, 1991; Stone, 2000) and the default ("global") production rate (Table 1).

Four samples were collected on the inward sloping crater walls to determine an age for the maar-forming eruption. Three of these (TA15-

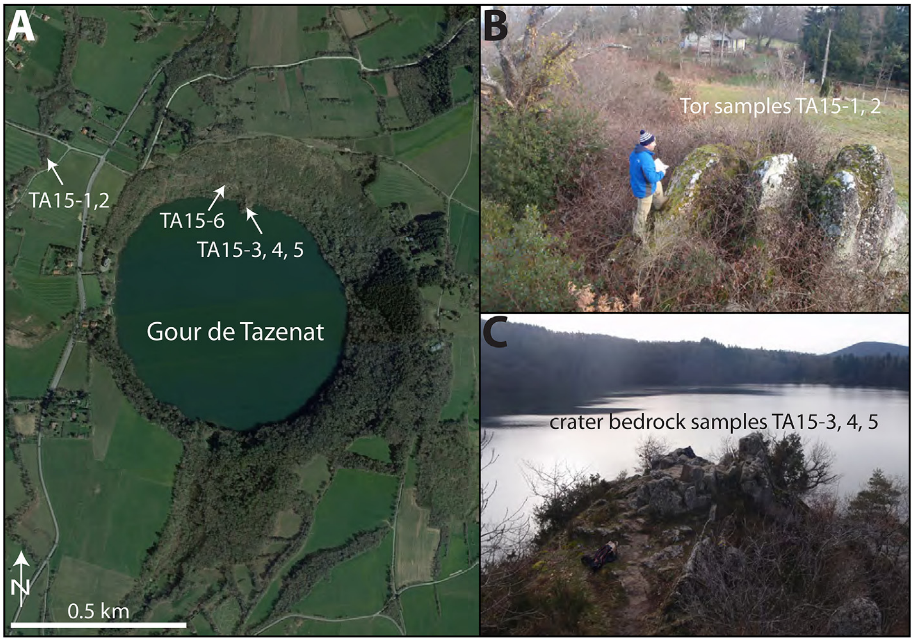

Fig. 3. A. Areal photograph of Gour de Tazenat and sample locations. **B.** Tor sample locations. **C.** Sample collection sites on peninsula within the crater.

3, −4, and −5, Fig. 3) were collected along a 15-m-long transect atop a bedrock peninsula that projects into the crater lake's northern side. This bedrock surface is inferred to have been first exposed during crater formation, as it juts out from the rest of the crater. The top of the peninsula is ~10 m above the current lake level, which is controlled by a natural outlet into Rochegude stream at its southwestern shore. It is likely that the lake has not greatly exceeded its current level in the time since the eruption, as there is no evidence that the outlet elevation has changed significantly because there has been little incision of the stream's bedrock channel. For this reason, the three sample sites on the northern peninsula have probably not been previously submerged by the crater lake. The peninsula was almost certainly covered by coarse tephra immediately after the eruption, but its position as a steep-sided, topographic high jutting into a crater makes it likely that these deposits were eroded off relatively quickly, thus we interpret the ^{10}Be ages as being a close minimum age for crater formation.

The fourth crater wall sample was taken from a higher elevation, where a Manzat Formation outcrop a few square meters in size forms a small ledge (sample TA15-6; Fig. 3a) on what is otherwise a relatively smooth slope from the lake to the crater rim. The altitude of this site is ~10 m above that of the peninsula samples described above, at about the same elevation as the sample sites on the tor described below, and might represent a paleohigh just prior to the maar-forming eruption. Unlike the peninsula samples, we are less confident that this surface has been exposed continuously since the eruption due to its proximity to the contact between bedrock and tephra ring deposits (within a few meters above the site).

Two additional samples were collected on a microgranite tor surface located outside the crater with the aim to constrain maximum exhumation rates for the maar's immediate surroundings, which can be used to refine the ages obtained within the crater to account for erosion of the sampled surfaces since their original exposure. The 7-m-high tor is located ~250 m northwest of the Tazenat crater rim, on otherwise low-relief terrain. Two samples (TA15-1, −2; Fig. 3a and b) were collected on the tor's top surface, separated by a horizontal distance of 6 m. Their apparent ^{10}Be ages (Table 1) are 125.1 ± 11.3 ka and 115.4 ± 10.5 ka. We applied the concept that the maximum ^{10}Be inventory in any Earth surface is a function of the rate of rock surface lowering of that surface (Bierman, 1994). In other words, the ^{10}Be inventory reaches saturation as a function of local erosion rate. For ancient surfaces exposed for long durations (10s to 100s kyr), where it can be assumed that the maximum ^{10}Be inventory has been reached, the ^{10}Be concentration can be inverted for the rate of surface lowering. Because it is unknown whether or not saturation has indeed been reached, resultant erosion rates are maximum estimates. Based on our two samples, we calculate maximum microgranite surface erosion rates of 5.1 ± 0.5 and 5.5 ± 0.6 m/Myr, averaging 5.3 ± 0.3 m/Myr.

As corroboration, our calculated maximum erosion rate of ~5.3 m/Myr is in general agreement with long-term erosion rates obtained from the approximations from inverted relief on the Plateau des Domes. A long, inverted-relief ridge of Miocene basanite lava, located ~5 km south of Gour de Tazenat, forms the Roche de Sauternes Ridge (Fig. 1). Lava that caps this ridge now lies 150 m above the base plateau level at its source and 180 m above at its lower end. Similarly, the Flateuf ridge

Table 1
Beryllium-10 sample information and age results.

Sample name	Latitude (N)	Longitude (E)	Elevation (m asl)	Thickness (cm)	Density (g cm^{-3})	Shielding correction	Erosion rate (cm yr^{-1})	[^{10}Be] atoms g^{-1}	Zero erosion age (years)	Erosion age (years)
TA15-1	45.98521°	2.98566°	654	3.0	2.65	1.0000	NA	856506.7 ± 17666.03	NA	NA
TA15-2	45.98521°	2.98566°	653	3.0	2.65	0.9980	NA	790134.8 ± 19043.74	NA	NA
TA15-3	45.98323°	2.99230°	643	5.0	2.65	0.9850	0.0005285	184383.4 ± 5192.929	27,308 ± 2815	31,168 ± 3699
TA15-4	45.98310°	2.99231°	641	3.5	2.65	0.9865	0.0005285	214191.9 ± 7649.051	31,415 ± 3317	36,686 ± 4577
TA15-5	45.98310°	2.99231°	641	3.5	2.65	0.9865	0.0005285	199777.3 ± 6051.391	29,345 ± 3043	33,871 ± 4094
TA15-6	45.98370°	2.99170°	653	2.0	2.65	0.9935	0.0005285	85258.36 ± 4629.699	12,101 ± 1364	12,784 ± 1525

Note. Be standard 07KNSTD, uncertainty includes AMS and production rate uncertainty, process blank ^{10}Be/^{9}Be ratio = 3.2 ± 0.2 × 10^{-14}.

in the south of the Chaîne des Puys is about 50 m higher than its surroundings. The ages of the lavas are approximately known from radiometric dating and field relationships (e.g. Guérin, 1983; Boivin et al., 2017) and their height above the current surroundings allows geomorphic estimation of regional exhumation rates on the terrain surrounding the Limagne Rift. These topographic and age relationships suggest an exhumation rate of ~5 m/Ma on the Plateau des Domes. This value is similar to the rate we calculate using the ^{10}Be data. Note that exhumation rates on the Limagne plain (within the rift; Fig. 1) are higher than this because of the relatively easily eroded sedimentary fill of the rift.

The raw ^{10}Be ages (not corrected for any surface erosion) for the peninsula samples within the crater (TA15-3,4,5; Table 1) are 27.3 ± 2.8, 29.3 ± 3.0 and 31.4 ± 3.3 ka, which average 29.4 ± 2.1 ka (Table 1). Applying the maximum bedrock surface erosion rate inferred from ^{10}Be measurements on the tor to the bedrock surfaces within the crater yields corrected ^{10}Be ages of 31.2 ± 3.7, 33.9 ± 4.1 and 36.7 ± 4.6 ka, which average 33.9 ± 2.8 ka (Table 1). It is possible that the surface erosion rate of the tor is higher than it is for fresh bedrock, thus the erosion-corrected ages are interpreted as maximum ages for the bedrock surfaces. In any case, our best estimate is that Gour de Tazenat was formed by an eruption between 29 and 34 ka. Sample TA15-6 yields a younger ^{10}Be age of 12.8 ± 1.5 ka (Table 1) is consistent with it having been covered by tephra for a substantial time after the eruption as suggested by the sample setting described above.

5. Conclusions

We used ^{10}Be dating on silicic bedrock exposed by crater formation to estimate that the Gour de Tazenat maar-forming eruption occurred between 29 and 34 ka. This accounts for bedrock surface erosion rates of ≤5.3 m/Ma constrained by ^{10}Be measurements from samples collected from a tor outside the crater, and corroborated by landscape exhumation rates determined by age and elevation relationships of inverted terrain in the area. Our age estimate for the formation of the maar is similar to the projected basal age of the sediment infill of ~35 cal ka (Juvigné and Bastin, 1995).

Volcanic hazard assessment in a volcanic field such as Chaîne des Puys, which is dominated by monogenetic volcanoes scattered over a broad area, requires knowledge of the time and space history of volcanism (e.g., Valentine and Connor, 2015). Our age estimate for the relatively isolated Gour de Tazenat show that it is significantly younger than the maars nearest to it, such as Beaunit maar (~9 km to the south-southeast), which dates to 54 ± 7 ka (Boivin et al., 2017). However, Gour de Tazenat erupted during a major phase of activity in the Chaîne des Puys, which took place over a few thousand years around 30,000 years B.P. During this time volcanoes in the central part of the volcanic field, such as Charmont, Petit Sarcoui, Paugnat, Lemptégy, and Puys de Gouttes were erupted (Fig. 1a; Boivin et al., 2009, 2017) Jumes and Coquille cones, which have similar morphological preservation, may also be from this phase. Thus, this ~30 ka pulse seems to have concerned a large areal portion of the Chaîne des Puys, at least from the central to the extreme northern end, which must be factored into future hazard assessments. In addition to providing eruption age information that can be used in studies of the Chaîne des Puys volcanic field and its potential hazards, this work demonstrates further potential usefulness of ^{10}Be dating for volcanic landforms.

Acknowledgements

We thank Didier Miallier and Pierre Boivin for informative discussions, and to Etienne Juvigné for sharing his knowledge of the outcrops around the Gour, especially his observations on the base of the Gour sequence and its palaeoclimatology implications. Constantin D. Athanassas and an anonymous reviewer provided very helpful comments that improved the manuscript. Fieldwork was conducted while Valentine was ClerVolc Visiting Professor at the Université Clermont Auvergne.

Appendix A. Supplementary data

Supplementary data associated with this article can be found, in the online version, at https://doi.org/10.1016/j.quageo.2018.11.002.

References

Balco, G., Stone, J.O., Lifton, N.A., Dunai, T.J., 2008. A complete and easily accessible means of calculating surface exposure ages or erosion rates from ^{10}Be and ^{26}Al measurements. Quat. Geochronol. 3, 174–195. https://doi.org/10.1016/j.quageo.2007.12.001.
Bierman, P.R., 1994. Using in situ produced cosmogenic isotopes to estimate rates of landscape evolution: a review from the geomorphic perspective. J. Geophys. Res. Solid Earth 99, 13885–13896.
Boivin, P., Besson, J.-C., Briot, D., Gourgaud, A., Labazuy, P., Langlois, E., de Larouzière, F.-D., Livet, M., Mergoil, J., Miallier, D., Morel, J.-M., Vernet, G., Vincent, P., 2009. Volcanologie de la Chaîne des Puys, fifth ed. Parc Naturel Regional des Volcans d'Auvergne 196 pp.
Boivin, P., Besson, J.C., Briot, D., Deniel, C., Gourgaud, A., Labazuy, P., Langlois, E., de Larouzière, F.D., Livet, M., Merciecca, C., Médard, E., Mergoil, J., Miallier, D., Morel, J.M., Thouret, J.V., Vernet, G., 2017. Volcanologie de la Chaîne des Puys, Massif Central, Français, sixth ed. Parc Naturel Régional des Volcans d'Auvergne 200 pp.
Camus, G., de Goër de Hervé, A., Kieffer, G., Mergoil, J., Vincent, P.M., 1983. Volcanologie de la Chaîne des Puys (Massif Central Français), second ed. Parc Naturel Regional des Volcanos d'Auvergne 112 pp.
Chassiot, L., Miras, Y., Chapron, E., Devellee, A.-L., Arnaude, F., Motelica-Heino, M., Di Giovanni, C., 2018. A 7000-year environmental history and soil erosion record inferred from the deep sediments of Lake Pavin (Massif Central, France). Palaeogeogr. Palaeoclimatol. Palaeoecol. 497, 218–233. https://doi.org/10.1016/j.paleo.2018.02.024.
Corbett, L.B., Bierman, P.R., Rood, D.H., 2016. An approach for optimizing in situ cosmogenic ^{10}Be sample preparation. Quat. Geochronol. 33, 24–34. https://doi.org/10.1016/j.quageo.20016.02.001.
Demarest, N., 1774. Mémoire sur l'origine et la nature du basalte à grandes colonnes polygones, déterminées par l'histoire naturelle de cette pierre, observée en Auvergne. Histoire et mémoires de l'Académie Royale des Sciences, vol 1771. Année, Paris, pp. 705–775.
Glangeaud, P., 1913. La Chaîne des Puys. Serv des Cart Geologiques Francaises, vol 135. pp. 241–469.
Guérin, G., 1983. La thermoluminescence des plagioclases, method de datation du volcanisme. Thesis In: Applications au domaine volcanique français: Chaîne des Puys, Mont Dore et Cezallier, Bas Vivarais. Université Pierre et Marie Curié.
Heisinger, B., Lal, D., Jull, A., Kubik, P., Ivy-Ochs, S., Knie, K., Nolte, E., 2002a. Production of selected cosmogenic radionuclides by muons: 2. Capture of negative muons. Earth Planet Sci. Lett. 200, 357–369.
Heisinger, B., Lal, D., Jull, A., Kubik, P., Ivy-Ochs, S., Neumaier, S., Knie, K., Lazarev, V., Nolte, E., 2002b. Production of selected cosmogenic radionuclides by muons 1. Fast muons. Earth Planet Sci. Lett. 200, 345–355.
Jeambrun, M., Giot, D., Alsac, C., 1986. *Carte géologique de la France à 1:50 000*. 669. Aigueperse, Bureau de recherches géologiques et minières. Service géologique national France.
Juvigné, E., Bastin, B., 1995. The Gour de Tazenat and the Late Glacial to Boreal environmental changes in the northern Chaine des Puys. Comptes Rendus de l'Academie des Sciences. Serie 2, *Sciences de la Terre et des Planetes* 321, 993–999.
Juvigné, E., Stach-Czerniak, A., 1998. Étude sédimentologique et palynologique des depots lacustres tardeclaciers et holocénes du Gour de Tazenat (Massif Central, France). Quaternaire 9, 15–23. https://doi.org/10.3406/quate.1998.2102.
Kohl, C.P., Nishiizumi, K., 1992. Chemical isolation of quartz for measurement of in-situ -produced cosmogenic nuclides. Geochem. Cosmochim. Acta 56, 3583–3587.
Lal, D., 1991. Cosmic ray labeling of erosion surfaces: in situ nuclide production rates and erosion models. Earth Planet Sci. Lett. 104, 424–439.
Pilleyre, T., 1991. Thesis DU. Datation par thermoluminescence - Application à la chronologie des retombées volcaniques, vol 354 Univerisité de Clermont II, Clermont-Ferrand 175 p.
Preusser, F., Rufer, D., Schreurs, G., 2011. Direct dating of Quaternary phreatic maar eruptions by luminescence methods. Geology 39, 1135–1138. https://doi.org/10.1130/G32345.1.
Sasnett, P., Goehring, B.M., Christie-Blick, N., Schaefer, J.M., 2012. Do phreatomagmatic eruptions at Ubehebe Crater (Death Valley, California) relate to a wetter than present hydro-climate? Geophys. Res. Lett. 39, L02401. https://doi.org/10.1029/2011GL050130.
Scrope, G.P., 1825. Considerations on volcanoes: the probable causes of their phenomena, the laws which determine their march, the disposition of their products, and their connexion with the present state and past history of the globe. In: Leading to the Establishment of a New Theory of the Earth. London. Printed and Published by W. Phillips, George Yard, Lombard Street; Sold by W. & C. Tait, Edinburgh; and Hodges & McArthur, Dublin.
Stone, J.O., 2000. Air pressure and cosmogenic isotope production. J. Geophys. Res. Solid

Earth 105, 23753–23759. https://doi.org/10.1029/2000JB900181.
Valentine, G.A., Connor, C.B., 2015. Basaltic volcanic fields. In: Sigurdsson, H., Houghton, B., McNutt, S.R., Rymer, H., Stix, J. (Eds.), The Encyclopedia of Volcanoes, *second ed.*. Elsevier, pp. 423–439. https://doi.org/10.1016/B978-0-12-385938-9.00023-7.
Valentine, G.A., Cortés, J.A., Widom, E., Smith, E.I., Rasoazanamparany, C., Johnsen, R., Briner, J.P., Harp, A.G., Turrin, B., 2017. Lunar Crater volcanic field (Reveille and Pancake ranges, basin and range Province, Nevada, USA). Geosphere 13, 391–438. https://doi.org/10.1130/GES01428.1.